Journal of Enzyme Inhibition and Medicinal Chemistry, June 2007; 22(3): 343–350

Spectral analysis and *in vitro* cytotoxicity profiles of novel organotin(IV) esters of 2-maleimidopropanoic acid

M. I. KHAN[1], MUSA KALEEM BALOCH[1], & MUHAMMAD ASHFAQ[2]

[1]*Department of Chemistry, Gomal University, D.I. Khan, Pakistan, and* [2]*Department of Chemistry, Islamia University, Bahawalpur, Pakistan*

(Received 27 May 2006; in final form 22 August 2006)

Abstract

Six novel triorganotin(IV) 2-maleimidopropanoato complexes: $R_3SnOCOCH_3(CH)(COCH)_2$, (R: Me(**1**), Et(**2**), n-Pr(**3**), n-Bu(**4**), Ph(**5**), Bz(**6**) have been synthesized. Their solid-state configuration has been determined by FT IR and ^{119m}Sn Mössbauer spectroscopy. The tin(IV) atom is five-coordinated in all the complexes with 2-maleimidopropanoic acid behaving as a monoanionic bidentate ligand coordinating the tin(IV) atom through a chelating or bridging carboxylate group. The solution-state configuration has been elucidated by means of ^{1}H-, ^{13}C- and ^{119}Sn-NMR spectroscopy which assigned a tetrahedron. Elemental analysis and FAB MS data also supported a 1:1 metal to ligand stoichiometry. The title complexes have been screened *in vitro* for anti-tumour, anti-fungal, anti-leishmanial and urease inhibition activities and displayed promising results.

Keywords: *Triorganotin(IV), 2-maleimidopropanoic acid, urease inhibition, anti-tumour, anti-leishmanial, anti-fungal*

Introduction

Metal complexes generally and organotin(IV) compounds especially constitute an important class of compounds which find a number of daily life biomedical and commercial applications like wood preservatives, anti-fouling paints, agricultural fungicides etc. [1–4]. During the past few decades, pharmaceutical properties of organotin(IV) carboxylates have been investigated for their anti-tumour activity [5–9]. Generally, the toxicity of organotin(IV) complexes is influenced by the structure of the ligand and its ability to coordinate and the order of toxicity is $R_3SnR' > R_2SnR'_2 > RSnR'_3$ [10]. Organotin(IV) carboxylates containing biologically active ligands like amino acids and their derivatives have found considerable attention due to significant bioactivity [11–19]. Recently, we have reported organotin(IV) complexes of different N-protected amino acids, but triorganotin(IV) esters of 2-maleimidopropanoic acid have not yet been reported and deserve detailed investigation [19–23]. We are of the view that it was of interest to synthesize, characterize and assess the *in vitro* bio-potential and structure-activity-relationship of such complexes.

Experimental

Materials

2-Aminopropanoic acid, maleic anhydride, triethylamine, trimethyltin(IV) chloride, triethyltin(IV) chloride, tripropyltin(IV) chloride, tributyltin(IV) chloride and triphenyltin(IV) chloride were Sigma or Fluka products of analytical purity and used as such, while tribenzyltin(IV) chloride was prepared according to a reported procedure [24]. Solvents used during this work were dried as reported [25]. Jack bean and *Bacillus pasteurii* urease were obtained from Sigma–Aldrich.

Instrumentation

Elemental analyses (C, H, N) were performed on a Yanaco high-speed CHN analyzer; antipyrene was used as a reference, while the tin content was

Correspondence: M. I. Khan, Department of Chemistry, Gomal University, D.I. Khan, Pakistan. Tel: 92 966 750424. Fax: 92 966 750255. E-mail: chmikhan@hotmail.com

ISSN 1475-6366 print/ISSN 1475-6374 online © 2007 Informa UK Ltd.
DOI: 10.1080/14756360601073062

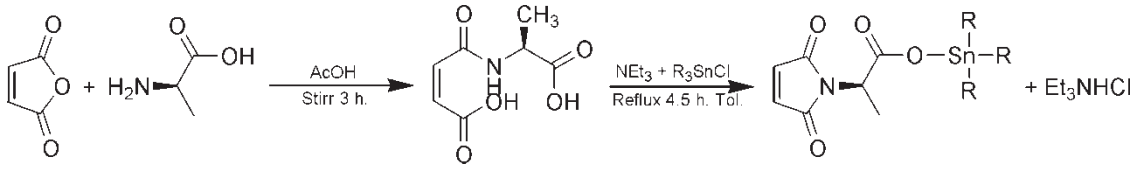

Scheme 1. Synthesis of organotin (IV) esters.

estimated according to reported procedures [26]. Uncorrected melting point was taken on a Reichert Thermovar (F. G. Bode Co., Austria).

The FT IR spectra of the pure solid samples were recorded on a Bruker FT IR spectrophotometer TENSOR27 (ZnSe) using OPUS software covering 5000–400 cm^{-1}.

For Mössbauer measurements, the solid samples were maintained by liquid nitrogen at a temperature of 77.3°K, using a V. G. Micromass 7070 F Cryolid liquid nitrogen cryostat. The multichannel calibration was performed with an enriched iron foil using ^{57}Co–Pd source, while the zero point of the Doppler velocity scale was determined through the absorption spectra of $CaSnO_3$ ($^{119}Sn = 0.5\,mg\,cm^{-2}$). The resulting 5×105 -count spectra were refined to obtain the isomeric shift, IS (mm s^{-1}), the nuclear quadrupole splitting QS, ρ (mm s^{-1}) and the width at half-height of the resonant peaks, Γ (mm s^{-1}).

^1H- and ^{13}C NMR spectra ($CDCl_3$) were recorded on a multinuclear Bruker *Biospin* AMX 300 MHz, FT NMR spectrometer using 300 and 75 MHz, respectively, at room temperature employing TMS as internal reference. ^{119}Sn NMR spectra in $CDCl_3$ were recorded at 186.50 MHz on a Bruker AMX 500 spectrophotometer using external neat $SnMe_4$ ($\delta\,^{119}Sn = 0$ ppm). EI mass spectra were recorded using a model MAT 112, Double-Focusing Mass Spectrometer (Finnigan).

Methods

Synthesis of 2-maleimidopropanoic acid. Maleic anhydride (10 g, 101.9782 mmoles) was dissolved in acetic acid (150 mL) and a cold solution of 2-aminopropanoic acid (9.0852 g, 101.9782 mmoles) in acetic acid (150 mL) added. The mixture was stirred at room temperature for 3 h resulting in a white precipitate which was washed thrice with cold water and recrystallized from water to get maleamic acid of analytical purity. Maleamic acid (5 g, 26.7165 mmoles) was suspended in dry toluene (350 mL), triethylamine (7.4806 mL, 53.433 mmoles) added and the suspension refluxed with rigorous stirring for 1.5 h with the concomitant removal of water using a Dean-Stark separator. The solvent was removed on a rotary evaporator (Büchi) leaving a hygroscopic solid; HCl was added up to pH 2 and the residue was extracted with ethyl acetate and the extract dried over anhydrous $MgSO_4$ and evaporated. The solid mass left was recrystallized from hexane (see Scheme I).

Synthesis of organotin(IV) complexes of 2-maleimidopropanoic acid. A solution of the triethylammonium salt of 2-maleimidopropanoic acid (0.5 g, 2.9563 mmoles) in dry toluene (75 mL) was prepared and the appropriate amount of triorganotin(IV) chloride (2.9563 mmoles) was added. The mixture was heated to reflux for 4.5 h which resulted in turbidity due to the formation of triethylammonium hydrochloride, which was filtered off and the filtrate was evaporated on a rotary evaporator. The solid mass was dissolved in a mixture of $C_6H_6$and C_6H_{14} (1:1) and the compound was recrystallized from CH_2Cl_2 (Scheme I).

Partition coefficient, in vitro *anti-tumour, anti-leishmanial and anti-fungal activity*. Partition coefficient measurement; and the protocol for *in vitro* anti-tumour, anti-leishmanial and anti-fungal activity is described elsewhere [20–23].

Urease assay and inhibition. A reaction mixture containing 10 ul/mL of 20 mg/mL and 2.5 mg/mL, respectively, of Jack bean and *Bacillus pasteuri* ureases (Sigma, catalog numbers U1500 and U7127, respectively) and 10 μL of 0.01, 0.02, 0.05 and 0.1 mM of test compound (**1**–**7**) were incubated at 30°C for 15 min in 96-well plates and then 55 μL of buffers containing 100 mM urea were incubated for 15 min. Then, final urease activity was determined by measuring ammonia production using the indophenol method as described by Weatherburn [27]. Briefly, 45 μL each of phenol reagent (1% w/v phenol and 0.005% w/v sodium nitroprusside) and 70 μL of alkali reagent (0.5% w/v NaOH and 0.1% active chloride NaOCl) were added to each well. The increasing absorbance at 630 nm was measured after 50 min, using a microplate reader (Molecular Device, USA). All the reactions were performed in triplicate in a final volume 200 μL. The results were processed using SoftMax Pro software (Molecular Device, USA). All the assays were performed at pH 8.2 (0.01 M $K_2HPO_43H_2O$, 1 mM EDTA and 0.01 M LiCl). Percentage inhibitions were calculated from the formula $100 - [(OD_{testwell}/OD_{control}) \times 100]$. Thiourea was used as the standard inhibitor of urease.

Table I. Physical and analytical data for complexes **1**–**6** and the ligand **7**.

Cpd.	Mol. formula	M.P. (°C)	Yield (%)	Elemental analysis calculated (found)			
				%C	%H	%N	%Sn
(**1**)	$C_{10}H_{15}NO_4Sn$	95	81	36.18(36.02)	4.55(4.32)	4.22(4.10)	35.76(35.48)
(**2**)	$C_{13}H_{21}NO_4Sn$	82	77	41.75(41.38)	5.66(5.43)	3.76(3.65)	31.74(31.53)
(**3**)	$C_{16}H_{27}NO_4Sn$	Gel	83	46.18(46.05)	6.54(6.31)	3.37(3.22)	28.53(28.29)
(**4**)	$C_{19}H_{33}NO_4Sn$	133	86	49.81(49.57)	7.26(7.09)	3.06(2.95)	25.91(25.75)
(**5**)	$C_{25}H_{21}NO_4Sn$	178	88	57.95(57.76)	4.09(4.01)	2.70(2.49)	22.91(22.85)
(**6**)	$C_{28}H_{27}NO_4Sn$	145	88	60.03(59.87)	4.86(4.66)	2.50(2.32)	21.19(21.04)
(**7**)	$C_7H_7NO_4$	118	84	49.71(49.67)	4.17(4.15)	8.28(8.25)	–

Results and discussion

The complexes and the ligand were synthesized by the general procedure depicted in Scheme I. Analytical data for the complexes showed metal/ligand 1:1 stoichiometry. All the compounds were quite stable, obtained in good yield (77–88%) and were soluble in most organic solvents. Elemental analysis data found were in good agreement with calculated data. The physical and analytical data for the investigated compounds are reported in Table I.

Solid state FT IR and ^{119m}Sn Mössbauer spectroscopic results

Diagnostically important vibrational bands like $\nu(COO)_{asym}$, $\nu(COO)_{sym}$, ν(Sn—C) and ν(Sn—O) were assigned in the spectral range 1700–400 cm^{-1} and are presented in Table II for **1**–**7**. The complexation of the tin(IV) with the ligand was confirmed by the presence of Sn—O and Sn—C bands in the range of 426–451 cm^{-1} and 521–540 cm^{-1} respectively. In the IR spectra of **7**, a broad band at 3200–2800 cm^{-1} for —COOH was observed which was absent in the spectra of **1**–**6**. Based on the difference, $\Delta\nu$ between $\nu(COO)_{sym}$ and $\nu(COO)_{asym}$ and the corresponding band position, it is proposed that the carboxylate group acted as a bidentate in all these complexes [28]. It is reported in the literature that $\Delta\nu$ values > 200 and < 350 cm^{-1} reflected the bidentate coordination in chain structures formed by bridging carboxylate groups for **1**–**6** (Figure 1a) [19,21]. Moreover, a characteristic sharp peak at 450 cm^{-1} was seen in the spectrum of **5** which also confirmed the Sn—Ph linkage (Table II) [29]. ^{119m}Sn Mössbauer parameters (QS, IS, Γ_1 and Γ_2) are also

Table II. FT IR data for complexes **1**–**6** and ligand **7** (cm^{-1}).

Comp.	$\nu(COO)_{asym}$	$\nu(COO)_{sym}$	$\Delta\nu$	ν(Sn—C)	ν(O—Sn)
(**1**)	1590	1387	203	521	461
(**2**)	1596	1372	224	526	414
(**3**)	1580	1371	209	531	445
(**4**)	1574	1365	209	522	437
(**5**)	1588	1369	219	540	432
(**6**)	1574	1370	204	525	426
(**7**)	1695	1357	338	–	–

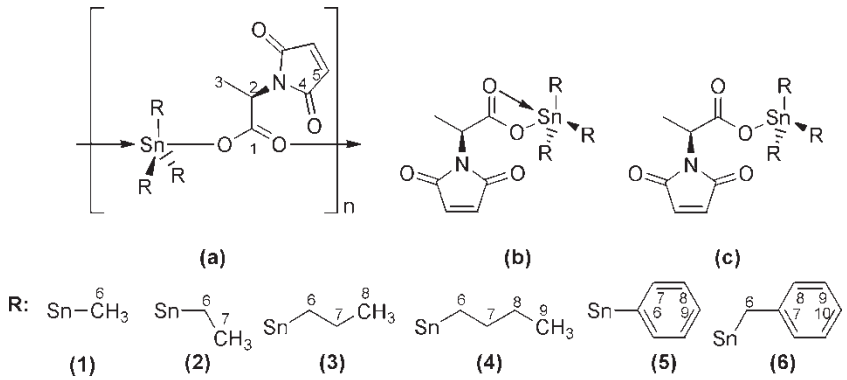

Figure 1. (a) Polymeric geometry, (b) tetrahedral geometry, (c) trigonal bipyrmidal geometry and numbering scheme for NMR.

Table III. ^{119m}Sn Mössbauer spectral data for complexes **1**–**6** (mm s^{-1}).

Compound	QS	IS	Γ_1	Γ_2	ρ = QS/IS
(**1**)	3.57	1.31	0.91	0.89	2.72
(**2**)	3.56	1.29	0.82	0.80	2.69
(**3**)	3.52	1.41	0.84	0.78	2.50
(**4**)	3.60	1.36	0.97	0.92	2.64
(**5**)	3.67	1.29	0.99	0.73	2.84
(**6**)	3.04	1.48	0.96	0.87	2.05

helpful in the determination of the solid-state configuration of organotin(IV) carboxylates [15–18]. ^{119m}Sn Mössbauer spectra of **1**–**5** showed quadrupole splitting (QS) value > 3.50 mms^{-1}; literature reveals that triorganotin(IV) esters having QS value > 3 mms^{-1} have a five coordinate chain structure formed by bridging carboxylate groups (Table III, Figure 1a) [30]. On the other hand, **6** displayed QS values 3.04 mms^{-1}, which recommended trigonal bipyramidal geometry (Figure 1b) [31]. On the basis of FT IR and Mössbauer spectra, it was concluded that **1**–**5** were bridged polymers, while **6** displayed cis-trigonal bipyramidal geometry in the solid phase.

Solution state ^{1}H- ^{13}C- and ^{119}Sn-NMR spectroscopic results

The ^{1}H NMR parameters of the organotin(IV) derivatives of 2-maleimidopropanoic acid are shown in Table IV. The integrated intensities of the spectra clearly indicated a 1:1 metal-to-ligand stoichiometry in solution, in agreement with the analytical data on the solids. Tin satellites were observed from which the coupling constants to tin can be obtained. Lockhart's equations (Equations (1) and (2)) using $^1\mathcal{J}$[^{119}Sn-^{13}C] and $^2\mathcal{J}$[^{119}Sn-^{1}H] values respectively were successfully applied to **1**–**4** for the determination of the C—Sn—C angle, θ [32] (Tables IV and V).

$$\theta = 0.0161|^2\mathcal{J}(^{119}\mathrm{Sn},^1\mathrm{H})|^2 - 1.32|^2\mathcal{J}(^{119}\mathrm{Sn},^1\mathrm{H})| + 133.4 \quad (1)$$

$$|^1\mathcal{J}(^{119}\mathrm{Sn},^{13}\mathrm{C})| = 11.4(\theta) - 875 \quad (2)$$

θC—Sn—C derived from Equations (1) and (2), for **1**–**4** had values of 110°, 108°, 112°, 111° and 111°, 108°, 111°, 108° respectively which confirmed that the hyper-coordination to Sn(IV) was lost in solution [33]. Moreover, $^1\mathcal{J}$[^{119}Sn-^{13}C] provided a trend $^1\mathcal{J} >> {}^2\mathcal{J} < {}^3\mathcal{J}$, which also indicated a tetrahedral environment of Sn(IV) [34]. These results clearly recommended a tetrahedral geometry for **1**–**4** [35]. ^{119}Sn NMR chemical shifts of **1**–**4** were typical of four-coordinated Sn(IV) complex; while for **5** and **6** peaks at 94.63 and −104.55 ppm indicated penta-coordination of Sn(IV). These results clearly indicated a tetrahedron for **1**–**4** and trigonal bipyramid for **5** and **6** in solution [21].

MS Spectrometry

FAB-MS substantiated the 1:1 metal-to-ligand stoichiometry and structural hypothesis based upon the aforementioned spectral analyses. The title complexes

Table IV. ^{1}H NMR data of **1**–**7** with $^2\mathcal{J}$(^{119}Sn-^{1}H) in parenthesis.

Proton	1	2	3	4	5	6	7
2	4.85q	4.91q	4.69q	4.77q	4.75q	4.71q	4.82q
3	1.72d	1.77d	1.68d	1.63d	1.60d	1.87d	1.78d
5	6.91s	6.87s	6.61s	6.92s	6.78s	6.99s	6.97s
6	0.14s(56)	0.95q(52)	0.74t(60)	0.85t(58)	–	2.76s(33)	–
7	–	0.76t	1.321m	1.61m	7.03m	–	–
8	–	–	1.13t	1.33m	7.00m	7.13m	–
9	–	–	–	0.89t	6.93m	7.31m	–
10	–	–	–	–	–	7.40m	–

Table V. ^{13}C NMR data of **1**–**7** with $^1\mathcal{J}$(^{119}Sn-^{13}C) in parenthesis.

Carbon	**1**	**2**	**3**	**4**	**5**	**6**	**7**
1	179.87	171.45	175.69	180.36	165.87	171.23	170.34
2	54.21	53.69	55.02	54.33	53.44	53.67	53.55
3	17.11	18.27	18.45	17.02	16.89	17.33	17.42
4	169.88	165.22	163.34	167.41	168.47	168.24	167.31
5	135.62	138.41	137.20	139.79	136.97	137.11	137.25
6	−2.13(393)	4.5(371)	20.43(403)	16.74(366)	140(687)	20.35(638)	–
7	–	12.34(44)	17.04(13)	27.4(18)	136(63)	139.5(16)	–
8	–	_	19.25(67)	27.95(60)	128.3(85)	123.6(28)	–
9	–	_	–	11.47	126.7(07)	131.4(40)	–
10	–	_	–	–	–	119.7	–
^{119}**Sn**	136.14	117.3	104.46	113.67	−94.63	−104.55	

Table VI. *In vitro* inhibition doses ID_{50} (ng/mL) of compounds **1**–**7** against seven tumoral cell lines of human origin.

	A498	EVSAT	H226	IGROV	M19	MCF7	WiDr
1	222	147	178	255	150	24	361
2	122	145	158	29	177	255	331
3	144	122	255	89	111	158	165
4	36	66	21	112	140	21	187
5	144	20	174	15	08	23	100
6	22	71	128	36	41	28	89
7	336	214	325	258	333	273	239
Do	28	44	68	107	23	35	62
Cp	1432	658	471	478	321	214	105
5-Fu	2214	325	164	205	301	54	82
Mt	3094	210	65	25	212	100	64
Et	514	531	438	328	155	84	103

cell lines: A498 (renal cancer), EVSA-T (mammary cancer), H226 (lung cancer), IGROV (ovarian cancer), M19 (melanoma), MCF-7 (mammary cancer) and WiDr (colon cancer); *reference drugs*: Do (doxorubicin), Cp (cisplatin), 5-Fu (5-fluorouracil), Mt (methotrexate) and Et (etopside).

followed a fragmentation pattern as earlier reported [19,23]. The base peak for **1**, **4** and **5** was due to the $[LSnR_2]^+$ fragment at m/z 317, 401, 441, respectively; while in **2**, **3** and **6** the $[LBSnR]^+$ fragment was at m/z 318, 330 and 378 [36].

Bioactivity

Compounds **1**–**7** were tested *in vitro* for their bioavailability, against seven human tumoural cell lines, five human pathogenic fungi and the urease enzyme. Table VI lists the concentration that inhibits 50% of the cell growth (ID_{50}) for 2-maleimidopropanoic acid (**7**) and its tin(IV) complexes (**1**–**7**) against A498 renal cancer, EVSA-T mammary cancer, H226 lung cancer, IGROV ovarian cancer, M19 melanoma, MCF-7 mammary cancer and WiDr colon cancer of human tumour origin along with the corresponding ID_{50} values for the clinically used drugs doxorubicin, cisplatin, 5-fluorouracil, methotrexate and etopside for comparison. All the complexes displayed significant activities in comparison to the ligand and the reference drugs, however, **5** and **6** were found to be the most potent.

Table VII represents concentrations of compounds **1**–**6** inducing 50% (IC_{50}) and 100% (IC_{100}) mortality for five leishmanial strains. It is quite evident from the data obtained that the complexes displayed significant activities in comparison to the ligand.

Promising results were observed during *in vitro* antifungal screening. The complexes **1**–**6** were more effective than the ligand **7**. The order of *in vitro* antifungal effectiveness is **6** > **5** > **4** > **3** > **2** > **1** > > **7**. The effect of dose over percent inhibition was plotted and from that graph we have determined the Optimum Dose by extrapolating the value up to the extent that a further increase in dose does not effect the inhibition (Table VIII). The results show a similar trend as their toxicity leading to the conclusion concludes that the higher the toxicity of a compound the lower is the optimum dose.

Table IX shows the inhibitory of **1**–**7** on urease. It was observed that compounds **5** and **6** displayed a potent inhibitory effect, **3** and **4** were moderate inhibitors while **1**, **2** and **7** were weak inhibitors of urease.

The bulkiness of R groups attached to Sn(IV), affected *in vitro* toxicity against the tumoural cell lines used. To highlight this statement, the average ID_{50} data have been plotted versus the percent CH in Figure 2. The percent CH has been defined as:

$$\text{Percent CH(R)} = [C_n(12.011) + H_n(1.0079)/\text{Molecular mass of the complex}] \times 100$$

Table VII. *In vitro* anti-leishmanial effect of **1**–**7** (mM) in promastigote stage.

	Anti-leishmanial IC_{50}/IC_{100}				
Compound	*L. major*	*L major* (Pak.)	*L. tropica*	*L. mex mex*	*L. donovani*
(**1**)	0.42/0.74	0.44/1.08	0.62/0.74	0.96/0.74	0.42/0.74
(**2**)	0.41/0.81	0.43/0.97	0.53/0.89	0.55/1.03	0.36/1.23
(**3**)	0.40/1.31	0.32/0.88	0.42/0.77	0.33/0.85	0.32/0.73
(**4**)	0.29/0.98	0.28/0.66	0.33/0.53	0.22/0.71	0.30/0.44
(**5**)	0.22/1.02	0.19/0.36	0.21/0.22	0.18/0.54	0.33/0.31
(**6**)	0.07/0.32	0.10/0.25	0.22/0.14	0.09/0.33	0.04/0.29
(**7**)	0.97/1.65	1.12/1.33	0.98/1.87	1.05/1.32	1.11/1.25

Table VIII. *In vitro* anti-fungal effect of **1**–**7**.

	% Inhibition @ 0.01, 0.02, 0.05, 0.1 mM						
Fungi	(1)	(2)	(3)	(4)	(5)	(6)	(7)
A	25,28,33,41	33,31,36,40	31,44,52,51	44,22,22,45	56,64,61,72	77,85,88,89	10,23,22,31
B	33,38,39,51	41,43,56,62	35,40,52,63	37,41,33,55	57,61,70,73	65,66,70,71	12,11,22,20
C	08,11,15,22	22,21,42,55	09,18,44,53	36,20,31,39	22,44,38,54	88,90,98,100	11,36,08,01
D	10,28,39,55	22,29,41,45	36,39,66,71	30,39,59,74	23,55,63,74	24,28,29,100	22,28,31,30
E	02,09,14,22	28,29,33,32	44,45,58,88	45,63,65,71	66,68,71,74	66,68,69,73	33,32,39,44
F	33,38,39,51	41,43,56,62	35,40,52,63	37,41,33,55	57,61,70,73	65,66,70,71	12,11,22,20
G	08,11,15,22	22,21,42,55	09,18,44,53	36,20,31,39	22,44,38,54	88,90,98,100	11,36,08,01
H	10,28,39,55	22,29,41,45	36,39,66,71	30,39,59,74	23,55,63,74	24,28,29,100	22,28,31,30
I	02,09,14,22	28,29,33,32	44,45,58,88	45,63,65,71	66,68,71,74	66,68,69,73	33,32,39,44
Od	0.2199	0.1898	0.1514	0.1309	0.1100	0.0874	0.6089

Fungi: **A**–**I**: *Alternaria padwicki*, *Botryodiplodia theobromae*, *Colletotrichum mause 75*, *Colletotrichum mause 246*, *Colletotrichum mause*, *Colletotrichum gloeosporiodes 282*, *Pestalotiposis guepini*, *Phytopohothora palmivora*, *Phytopohothora palmivora*. *Od*: Optimum Dose.

Table IX. *In vitro* inhibition of urease by compounds **1**–**7**.

Compound	$IC_{50} \pm$ Sem (*Bacillus pasteurii* urease)	$IC_{50} \pm$ Sem (Jack bean urease)
1	76.04 ± 0.77	88.35 ± 0.41
2	71.55 ± 0.81	85.36 ± 0.66
3	55.33 ± 0.72	58.22 ± 0.31
4	40.64 ± 0.31	42.03 ± 0.01
5	11.25 ± 0.04	22.28 ± 0.35
6	9.15 ± 0.25	10.23 ± 0.11
7	66.92 ± 0.31	89.74 ± 0.04
Thiourea (Standard)	16.07 ± 0.78	22.35 ± 0.13

Standard mean error of 3–5 assays. All the IC_{50} values are in μM.

Where n is the number of carbon or hydrogen atoms in the R group.

In Figure 2, ID_{50} decreases almost linearly with the increase in percent CH. However, some deviations in the case of alkyl R groups have been observed, which may be attributed to variation in conformational behavior and distribution of complexes between phases.

Since it is difficult to judge the bioactivity of any compound by a single factor, we have tried another important parameter, the partition coefficient and the ID_{50} values have been plotted versus ID_{50} (see Figure 3). It is interesting to note that the data for complexes **1**–**6** show that the ID_{50} values decrease linearly with the increase in partition coefficient. It is certainly encouraging to us that the major controlling parameter seems to be P_{ow} (partition coefficient in octanol/water system) or, in other words, the polarizibility of the R′—Sn bond induced by R groups. It can be therefore be concluded that in complexes **1**–**6**, lipophillicity increases with the bulkiness of R groups, which enhances the partition coefficient, thereby increasing the bioactivity. Moreover, the

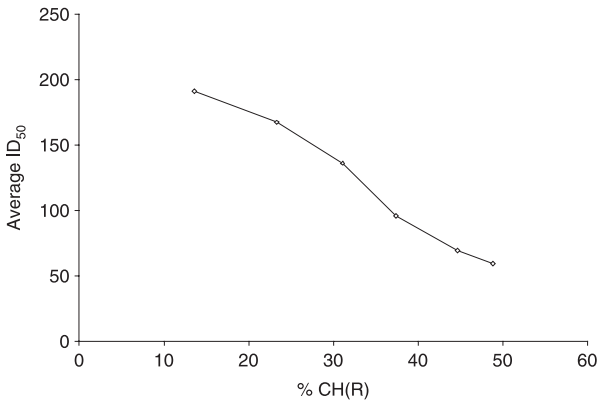

Figure 2. Dependence of *in vitro* anti-tumour ID_{50} on percent CH for complexes **1**–**6**.

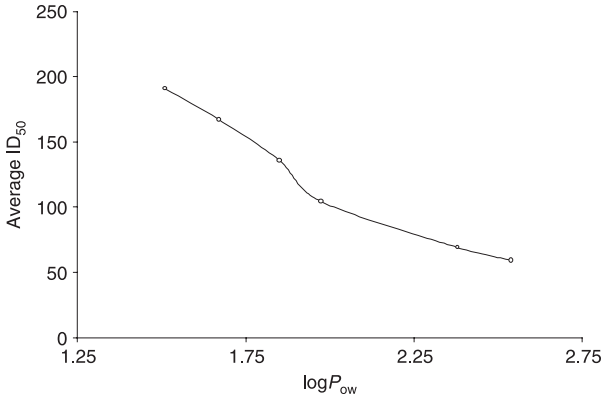

Figure 3. Dependence of *in vitro* anti-tumour ID_{50} on partition coefficients of complexes **1**–**6**.

polarity of Sn—C is also of the same order (Bz > Ph > Bu > Pr > Et > Me). In conclusion, we can say that the bulkiness of the attached R group/percent CH values and polar character of carboxylic group of 2-maleimidopropanoic acid are interlinked with each other, which enhance the polarity and partition coefficients of the complexes. A study is currently being carried out for the *in vivo* interactions/mechanism of action of these complexes.

Acknowledgements

This work was carried out with the financial support of Gomal University, D. I. Khan, Pakistan, (Research Project No. 717-29/DF/GU).

References

[1] Maqsood ZT, Khalid KM, Ashiq U, Jamal RA, Chohan ZH, Mahroof-Tahir M, Supuran CT. Oxovanadium(IV) complexes of hydrazides: Potential antifungal agents. J Enzyme Inhib Med Chem 2006;21:37. DOI:10.1080/14756360500277459j.jorganchem.2005.10.007T.

[2] Chohan ZH, Supuran CT. *In-vitro* antibacterial and cytotoxic activity of cobalt (II), copper (II), nickel (II) and zinc (II) complexes of the antibiotic drug cephalothin (Keflin). J Enzyme Inhib Med Chem 2005;20:463. DOI:10.1080/104852505002213280.

[3] Rehman SU, Chohan ZH, Gulnaz F, Supuran CT. *In-vitro* antibacterial, antifungal and cytotoxic activities of some coumarins and their metal complexes. J Enzyme Inhib Med Chem 2005;20:333. DOI:10.1080/14756360500141911.

[4] Lickiss PD In: Smith PJ, editor. Chemistry of tin. London: Blackie; 1998.

[5] Van Laar JAM, Rustam YM, Van der Vit C, Smid K, Kuiper CM, Pinedo HM, Peters GJ. Tumor size and origin determine the antitumor activity of cisplatin or 5-fluorouracil and its modulation by leucovorin in murine colon carcinomas. Cancer Chemother Pharmacol 1996; 39: 79.

[6] Girasolo MA, Schillaci D, Di Salvo C, Barone G, Silvestri A, Ruisi G. Synthesis, spectroscopic characterization and in vitro antimicrobial activity of diorganotin(IV) dichloride adducts with [1,2,4]triazolo-[1,5-a]pyrimidine and 5,7-dimethyl-[1,2,4]triazolo-[1,5-a]pyrimidine. J Organomet Chem 2005; 961:963. DOI:10.1016/j.jorganchem.2005.10.007.

[7] Ronconi L, Marzano C, Russo U, Sitran S, Graziani R, Fregona D. Synthesis, characterization and in vitro cytotoxicity of new organotin(IV) derivatives of N-methylglycine. J Inorg Biochem 2002;91:413. DOI:10.1016/ S0162-0134(02) 00465-8.

[8] Marchetti F, Pellei M, Pettinari C, Pettinari R, Rivarola E, Santini C, Skelton BW, White AH. Tin(IV) and organotin(IV) derivatives of bis(pyrazolyl)acetate: Synthesis, spectroscopic characterization and behaviour in solution.: X-ray single crystal study of bis(pyrazol-1-yl)acetatotri-iodotin(IV) [SnI3(bdmpza)]. J Organomet Chem 2005;690:1878. DOI:10.1016/j.jorganchem.2005.01.067.

[9] Thoonen SHL, Deelman B-J, van Koten G. Synthetic aspects of tetraorganotins and organotin(IV) halides. J Organomet Chem 2004;689:2145. DOI:10.1016/j.jorganchem.2004.03.027.

[10] Pellerito L, Nagy L. Organotin(IV)$^{n+}$ complexes formed with biologically active ligands: Equilibrium and structural studies, and some biological aspects. Coord Chem Rev 2002;224:111. DOI:10.1016/S0010-8545(01)00399-X.

[11] Meriem A, Gielen M, Willem R. Synthesis, characterization and antitumour activity of a series of diorganotin(IV) derivatives of bis(carboxymethyl)amines. J Organomet Chem 1989;365:91. DOI:10.1016/0022-328X(89)87170-0.

[12] Yin HD, Wang QB, Xue SC. Synthesis and spectroscopic properties of [N-(4-carboxyphenyl) salicylideneiminato] di- and tri-organotin (IV) complexes and crystal structures of $[^nBu_2Sn(2\text{-}OHC_6H_4CH{=}NC_6H_4COO)]_2O_2$ and $Ph_3Sn(2\text{-}OHC_6H_4CH{=}NC_6H_4COO)$. J Organomet Chem 2005; 690:435. DOI:10.1016/jjorganchem200409063.

[13] Zhou Y, Jiang T, Ren S, Yu J, Xia Z. Synthesis, crystal structure and in vitro antitumor activity of di-n-butyltin 4′-(7-oxabicyclo [2,2,1]-5-heptane-2,3-dicarboximide) benzoates. J Organomet Chem 2005;690:2186. DOI:10.1016/j.jorganchem.2005.01.062.

[14] Harrison PG, Sharpe NW. Complexes of terminally-protected dipeptides with trimethyltin as models for triorganotin-protein interactions. Inorg Chim Acta 1985;108:7. DOI:10.1016/S0020-1693(00)84315-7.

[15] Sandhu GK, Gupta R, Sandhu SS, Parish RV, Brown K. Diorganotin(IV) derivatives of N-phthaloyl amino acids. J Organomet Chem 1985;279:373. DOI:101016/0022-328X(85)87035-2.

[16] Sandhu GK, Gupta R, Sandhu SS, Parish RV. Diorganotin(VI) complexes of N-acetylamino acids. Polyhedron 1985;4:81. DOI:10.1016/S0277-5387(00)84226-6.

[17] Sandhu GL, Hundal R, Tiekink ERT. Structural chemistry of organotin carboxylates : XVII. Diorganotin(IV) derivatives of N-phthaloyl-DL-valine. J Organomet Chem 1992;430:15. DOI:10.1016/0022-328X(92)80091-B.

[18] Lo K-M, Kumar Das VG, Yip W-H, Mak TCW. Organotin esters of 3-ureidopropionic acid. Crystal structure of triphenyltin(IV) 3-ureidopropionate, $(C_6H_5)_3SnOCO(CH_2)_2NHCONH_2$. J Organomet Chem 1991;412:21. DOI:10.1016/0022-328X(91)86037-Q.

[19] Khan MI, Baloch MK, Ashfaq M, Peters GJ. *In vivo* toxicological effects and spectral studies of Organotin(IV) N-maleoylglycinates. Appl Organomet Chem 2005;19:132. DOI:10.1002/aoc807.

[20] Khan MI, Baloch MK, Ashfaq M. Biological aspects of new Organotin(IV) compounds of 3-maleimidopropionic acid. J Organomet Chem 2004;689:3370. DOI:10.1016/j.jorgan.chem.2003.10.007.

[21] Ashfaq M, Khan MI, Baloch MK, Malik A. Biologically potent Organotin(IV) complexes of 2-maleimidoacetic acid. J Organomet Chem 2004;689:238. DOI:10.1016/j.jorganchem.2003.10.007.

[22] Khan MI, Baloch MK, Ashfaq M, Obaidullah. Synthesis, characterization and *in vitro* cytotoxic effects of new organotin(IV)-2-maleimidopropanoates. Appl Organomet Chem 2006; 20:463. DOI:10.1002/aoc1083.

[23] Khan MI, Baloch MK, Ashfaq M, Stoter G. *In vivo* toxicological effects and spectral studies of new triorganotin(IV)-N-maleoyltranexamates. J Organomet Chem 2006; 691:2554. DOI:10.1016/j.jorganchem.2006.01.057.

[24] Sisido K, Takeda Y, Kinugawa Z. Direct Synthesis of Organotin Compounds. I. Di- and Tribenzyltin Chlorides. J Am Chem Soc 1961; 83:538.

[25] Furniss B, Hannaford AJ, Smith PWG, Tatchell AR. Vogel's text book of practical organic chemistry. UK: ELBS Longman Group; 1989.

[26] Mendham J, Denney RC, Barnes JD, Thomas M. Vogel's text book of quantitative chemical analysis. Singapore: Pearson Education Pte. Ltd; 2003.

[27] Weatherburn MW. Phenol-hypochlorite reaction for determination of ammonia. Anal Chem 1967;39:971. DOI: 10.1021/ac60252a045.

[28] Lebl T, Holecek J, Lycka A. Sci Pap Univ Pardubice Ser 1996; 5:A2.

[29] Whiffen DH. Vibrational frequencies and thermodynamic properties of fluoro-, chloro-, bromo and iodo-benzene. J Chem Soc 1956;1350. DOI:10.1039/ JR9560001350.

[30] Smith PJ, Day RO, Chandrasekhar V, Holmes JM, Holmes RR. Pentacoordinated molecules. 66. Chain structures of trimethyltin esters of salicylic acid and o-anisic acid. Tin-119m Moessbauer study of a series of trimethyltin and triphenyltin carboxylates. Inorg Chem 1984;25:2495. DOI: 10.1021/ ic00235a005.

[31] Sharma HK, Lata S, Sharma KK. Molloy KC,Waterfield PC. Synthesis and spectroscopic studies on dibutyl-, tributyl- and triphenyltin esters of *p*-methoxy *trans*-cinnamic acid. J Organomet Chem 1988;315:9. DOI: 10.1016/0022-328X (88)80294-8.

[32] Lockhart TP, Manders WF, Holt EM. Metal-stabilized rare tautomers of nucleobases. 1. Iminooxo form of cytosine: Formation through metal migration and estimation of the geometry of the free tautomer. J Am Chem Soc 1986; 108:6611. DOI: 10.1021/ja00281a027.

[33] Willem R, Bouhdid A, Mahieu B, Ghys L, Biesemans M, Tiekink ERT, Vos D de, Gielen M. Synthesis, characterization and *in vitro* antitumour activity of triphenyl- and tri-*n*-butyltin benzoates, phenylacetates and cinnamates. J Organomet Chem 1997; 531–151. DOI: 10.1016/S0022-328X(96)06686-7.

[34] Dalil H. A novel approach to soluble polystyrenes functionalized by tri-*n*-butyltin carboxylates. Macromol Chem Phys 2000;201:1266. DOI: 10.1002/1521-3925(20000801)201: 12 < 1266::AID-MACP1266 > 3.0.CO;2-O.

[35] Pellerito A, Fiore T, Giuliani AM, Maggio F, Pellerito L, Vitturi R, Colomba MS, Barbieri R. Organometallic Complexes with Biological Molecules: VIII. Synthesis, Solid State and *in vivo* Investigation of Triorganotin(IV) Derivatives of L-Homocysteic Acid. Appl Organomet Chem 1997;11:601. DOI: 10.1002/(SICI)1099-0739(199707)11:7 > 601::AID-AOC616 > 3.0.CO;2-1.

[36] López-Torres E, Mendiola MA, Pastor CJ, Procopio JR. Diorganotin(iv) Complexes of a Cyclic Thiosemicarbazone Ligand: Crystal Structures of $[SnPh_2(C_{15}H_{10}N_3S)Cl]$ and $[SnMe_2(C_{15}H_{10}N_3S)_2]$. Eur J Inorg Chem 2003;2711. DOI: 10.1002/ejic.200300090.